Application of two-parameter dynamical replica theory to retrieval dynamics of associative memory with non-monotonic neurons

2001 J. Phys. A: Math. Gen. 34 2695

(http://iopscience.iop.org/0305-4470/34/13/303)

INSTITUTE OF PHYSICS PUBLISHING JOURNAL OF PHYSICS A: MATHEMATICAL AND GENERAL

J. Phys. A: Math. Gen. **34** (2001) 2695–2712 www.iop.org/Journals/ja PII: S0305-4470(01)17991-6

Application of two-parameter dynamical replica theory to retrieval dynamics of associative memory with non-monotonic neurons

Toshiyuki Tanaka[1], **Shinsuke Kakiya**[1] **and Masato Okada**[2]

[1] Department of Electronics and Information Engineering, Tokyo Metropolitan University, Tokyo, Japan
[2] Kawato Dynamic Brain Project, Japan Science and Technology Corporation, Kyoto, Japan

Received 10 October 2000, in final form 12 January 2001

Abstract

Two-parameter dynamical replica theory (2-DRT) is applied to investigate retrieval properties of non-monotonic associative memory, a model which lacks thermodynamic potential functions. 2-DRT reproduces the dynamical properties of the model quite well, including the capacity and basin of attraction. The super-retrieval state is also discussed in the framework of 2-DRT. The local stability condition of the super-retrieval state is given, which provides a better estimate of the region in which super-retrieval is observed experimentally than the self-consistent signal-to-noise analysis does.

PACS numbers: 0520, 0230, 8435

1. Introduction

The Hopfield model has attracted the interest of researchers in various fields, and enormous an amount of studies, both numerical-experimental and theoretical, have been carried out on it. Of particular interest among them is the one with the model possessing *non-monotonic* units [1]: whereas the conventional model uses, as the output function f of a unit, monotonic functions such as $f(x) = \tanh \beta x$ ($\beta > 0$), the model with non-monotonic units, or the non-monotonic model for short, uses a non-monotonic function. It has been reported that the non-monotonic model has various nice properties as a model of associative memory. These include enhancement of storage capacity and enlargement of basins of attraction associated with retrieval states.

In order to rigorously argue such properties of the non-monotonic model, theoretical analyses are necessary. However, attempts to analyse the non-monotonic model are often faced with difficulty because the non-monotonic model in general does not have a Lyapunov function, which would be a powerful analytical tool for characterizing the equilibrium as well as dynamical properties of the model. Thus, applicable theories are restricted to what have been devised for analysing the conventional model and yet are independent of the functional form of the output function f. As for equilibrium analysis, the self-consistent signal-to-noise

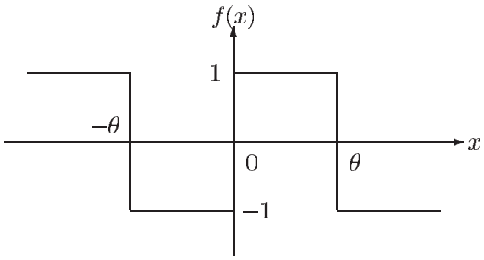

Figure 1. The non-monotonic function $f(x)$.

analysis (SCSNA) has been applied to the non-monotonic model [2] and some interesting properties, including the existence of the so-called super-retrieval states, have been found. For retrieval dynamics, on the other hand, currently no exact and tractable theory is known even for the conventional model: the path integral formalism [3] and Gardner–Derrida–Mottishaw theory [4] (for the 'zero-temperature', or $\beta \to +\infty$ case) are the exact theories for the asynchronous (or Glauber) and synchronous (or Little) dynamics, respectively, but computation of dynamics based on each of them is prohibitively difficult. It has been generally believed [3,5,6] that any tractable theories on retrieval dynamics necessarily incorporate some approximation. For the conventional model with the synchronous dynamics, Amari–Maginu theory [7] (for the zero-temperature case; for extension to the finite-temperature case, see [8]) has been proposed as one such theory, and Nishimori and Opriş [9] have applied it to the non-monotonic case. As one of the tractable theories for the conventional model with asynchronous dynamics, Coolen and Sherrington [10,11] have proposed a two-parameter dynamical replica theory (2-DRT hereafter; it is also sometimes called the Coolen–Sherrington (CS) theory). Of course it is an approximate theory, as confirmed, for example, by Ozeki and Nishimori [12] and Tanaka and Osawa [13]; nevertheless, it describes retrieval dynamics of the conventional model reasonably well. As Ozeki and Nishimori [12] have mentioned, formulation of 2-DRT does not depend on the functional form of the output function f, and therefore it is possible to apply it to the non-monotonic model. Thus, the following question naturally arises: *How well does 2-DRT describe retrieval dynamics of the non-monotonic model?* In this paper, we address this problem, with emphasis placed on the storage capacity, size of basins of attraction and the super-retrieval states.

2. Model

Let us consider a model with N units. Each unit has a binary variable $s_i \in \{-1, 1\}$, $i = 1, \ldots, N$, and $\boldsymbol{s} = [s_1, \ldots, s_N] \in \{-1, 1\}^N$ represents a microscopic state of the model. Each unit stochastically and asynchronously updates the value of s_i based on the current value of the 'local field':

$$h_i(\boldsymbol{s}) = \sum_{j \neq i} J_{ij} s_j \tag{1}$$

where J_{ij} is a synaptic weight from neuron j to neuron i. The probability of state flip $s_i := -s_i$ is given by the following transition probability:

$$w_i(\boldsymbol{s}) = \tfrac{1}{2}(1 - s_i f(h_i(\boldsymbol{s}))) \tag{2}$$

where $f : \boldsymbol{R} \mapsto [-1, 1]$ is the output function. Taking $f(x) = \tanh \beta x$ yields the conventional Hopfield model. In this paper we consider the following non-monotonic function (figure 1):

$$f(x) = \begin{cases} -\operatorname{sgn}(x) & (|x| \geqslant \theta) \\ \operatorname{sgn}(x) & (|x| < \theta). \end{cases} \tag{3}$$

Its functional form is the same as that treated by Nishimori and Opriş [9]. Throughout the paper, we follow the common timescale convention, which is taken in such a way that the average number per unit time (frequency) of updates each unit executes is one.

The model memorizes $p = \alpha N$ binary patterns $\boldsymbol{\xi}^\mu = [\xi_1^\mu, \ldots, \xi_N^\mu] \in \{-1, 1\}^N$, $\mu = 1, \ldots, p$, via the Hebb rule,

$$J_{ij} = \frac{1}{N} \sum_{\mu=1}^{p} \xi_i^\mu \xi_j^\mu \qquad (i \neq j). \tag{4}$$

The quantity $\alpha \equiv p/N$ is called the memory rate. We consider the case where the patterns to be memorized are randomly generated, that is, each ξ_i^μ takes the value ± 1 with probability $1/2$, independently of the others.

For measuring how well the model retrieves a pattern μ, the correlation, or overlap,

$$m^\mu(\boldsymbol{s}) = \frac{1}{N} \sum_{i=1}^{N} \xi_i^\mu s_i \tag{5}$$

is used: $|m^\mu(\boldsymbol{s})| \leqslant 1$ holds by definition, and if $m^\mu(\boldsymbol{s}) = 1$, then the model is in the state $\boldsymbol{s} = \boldsymbol{\xi}^\mu$, and it is regarded as perfectly retrieving the pattern μ. When $m^\mu(\boldsymbol{s}) = -1$ the model is in the state $\boldsymbol{s} = -\boldsymbol{\xi}^\mu$. The state is called the reversal state, but it can also be regarded as retrieving the pattern μ due to the symmetry of the model.

We assume that the model is going to retrieve a single pattern, so that $m^\mu(\boldsymbol{s})$ are of order unity for that pattern only (the *condensed ansatz*), and that pattern $\mu = 1$ is nominated for retrieval, without loss of generality. Then $m \equiv m^1(\boldsymbol{s})$ can be taken as a macroscopic variable, or order parameter, describing how well the model retrieves the nominated pattern. If the model reaches an equilibrium with $m \neq 0$, the model is said to successfully retrieve the pattern, and such an equilibrium is called a retrieval state. The local field $h_i(\boldsymbol{s})$ is now rewritten as

$$h_i(\boldsymbol{s}) = \xi_i^1 [m + z_i(\boldsymbol{s})] - \frac{1}{N} s_i \qquad z_i(\boldsymbol{s}) \equiv \xi_i^1 \sum_{\mu>1}^{p} \xi_i^\mu \frac{1}{N} \sum_{j \neq i} \xi_j^\mu s_j. \tag{6}$$

The term $z_i(\boldsymbol{s})$ represents the interference in the local field from non-nominated patterns $\mu > 1$, and is called the 'noise' term. Although time evolution of the microscopic state of the model is stochastic in nature, it is observed that the evolution of the order parameter m in the course of pattern retrieval can be often seen as being governed by a certain deterministic law. To describe the retrieval dynamics is one of important problems in this field. Path integral formalism [3] provides an exact description for the retrieval dynamics, but it requires parametrization with infinite degrees of freedom and is therefore practically intractable.

3. Two-parameter dynamical replica theory (2-DRT)

2-DRT, proposed by Coolen and Sherrington [10, 11], provides a tractable, and yet reasonably good description of the retrieval dynamics for the conventional model. It uses two parameters, m and r, as the order parameters, the latter being defined as

$$r \equiv \frac{1}{\alpha} \sum_{\mu>1} (m^\mu(\boldsymbol{s}))^2 \tag{7}$$

which intuitively represents the degree of the interferential effect of non-nominated patterns $\mu > 1$ onto the retrieval of pattern 1. 2-DRT derives deterministic flow equations for these two order parameters. Without any assumptions, one cannot expect that the flow equations for these two parameters are closed, and thus the time evolution of m and r cannot be completely

determined by their current values. In the framework of DRT in general, the following two assumptions are made:

(1) Self-averaging of flow equations with respect to the randomness of the system (randomly chosen patterns for the case treated in this paper).
(2) Probability equipartitioning within subshells: when values of the order parameters are given, the probability distribution of the corresponding microscopic state can be regarded as being uniform over the subshell (the set of microscopic states which have the specified values of the order parameters), with regard to calculation of the flow equations.

Owing to these closing assumptions, one can derive the deterministic flow equations for m and r:

$$\frac{\mathrm{d}m}{\mathrm{d}t} = \int \mathrm{d}z\ D_{m,r}[z]\ f(m+z) - m$$
$$\frac{1}{2}\frac{\mathrm{d}r}{\mathrm{d}t} = \frac{1}{\alpha}\int \mathrm{d}z\ D_{m,r}[z]\ zf(m+z) + 1 - r$$

where $D_{m,r}[z]$ is the distribution of the noise terms. Replica calculation gives, within the replica-symmetric (RS) ansatz, the RS solution $D^{\mathrm{RS}}_{m,r}[z]$ for the noise distribution, which has been derived by CS [10, 11] as

$$D^{\mathrm{RS}}_{m,r}[z] = \frac{\mathrm{e}^{-(\Delta+z)^2/2\alpha r}}{2\sqrt{2\pi\alpha r}}\left\{1 - \int Dy \tanh\left[\lambda y\left(\frac{\Delta}{\rho\alpha r}\right)^{1/2} + (\Delta+z)\rho\frac{r_{\mathrm{AGS}}}{r} + \mu\right]\right\}$$
$$+ \frac{\mathrm{e}^{-(\Delta-z)^2/2\alpha r}}{2\sqrt{2\pi\alpha r}}\left\{1 - \int Dy \tanh\left[\lambda y\left(\frac{\Delta}{\rho\alpha r}\right)^{1/2} + (\Delta-z)\rho\frac{r_{\mathrm{AGS}}}{r} - \mu\right]\right\} \tag{8}$$

$$\Delta = \rho\alpha(r - r_{\mathrm{AGS}}) \tag{9}$$

$$r_{\mathrm{AGS}} = \frac{\lambda^2}{\rho^2\alpha} \tag{10}$$

where $Dy = (\mathrm{d}y/\sqrt{2\pi})\mathrm{e}^{-y^2/2}$ is the Gaussian measure. The parameters $\{q,\ \lambda,\ \rho,\ \mu\}$ are to be determined from m, r, and α using the following saddle-point equations:

$$r = \frac{1-\rho(1-q)^2}{[1-\rho(1-q)]^2} \qquad \lambda = \frac{\rho\sqrt{\alpha q}}{1-\rho(1-q)}$$
$$m = \int Dy\ \tanh(\lambda y + \mu) \qquad q = \int Dy\ \tanh^2(\lambda y + \mu). \tag{11}$$

It should be noted that the replica calculation of the noise distribution bears no relation to the dynamics of the model and the choice of the output function f; it executes averaging over the (m, r)-subshell with uniform measure, and therefore the calculation is not dynamical but configurational. This is the reason why, apart from the validity of the two assumptions, 2-DRT can be straightforwardly applied to the non-monotonic model.

The latter of the two above-mentioned assumptions, the *equipartitioning* assumption, is a critical one because it has been known that it is not valid for the conventional model [13], as well as the continuous-valued linear system, or the Langevin spin system [14]. To show this directly for the conventional model, Tanaka and Osawa [13] have proposed a dynamics, called (m, r)-annealing. The (m, r)-annealing is defined, on the basis of the solution $\{\rho,\ \mu\}$ of the saddle-point equations for given m and r, as the dynamics of the conventional model with the inverse temperature ρ (that is, it uses $f(x) = \tanh \rho x$), but an extra bias is added to the local field,

$$h_i(\boldsymbol{s}) = \sum_{j\neq i} J_{ij}s_j + b\xi^1_i \tag{12}$$

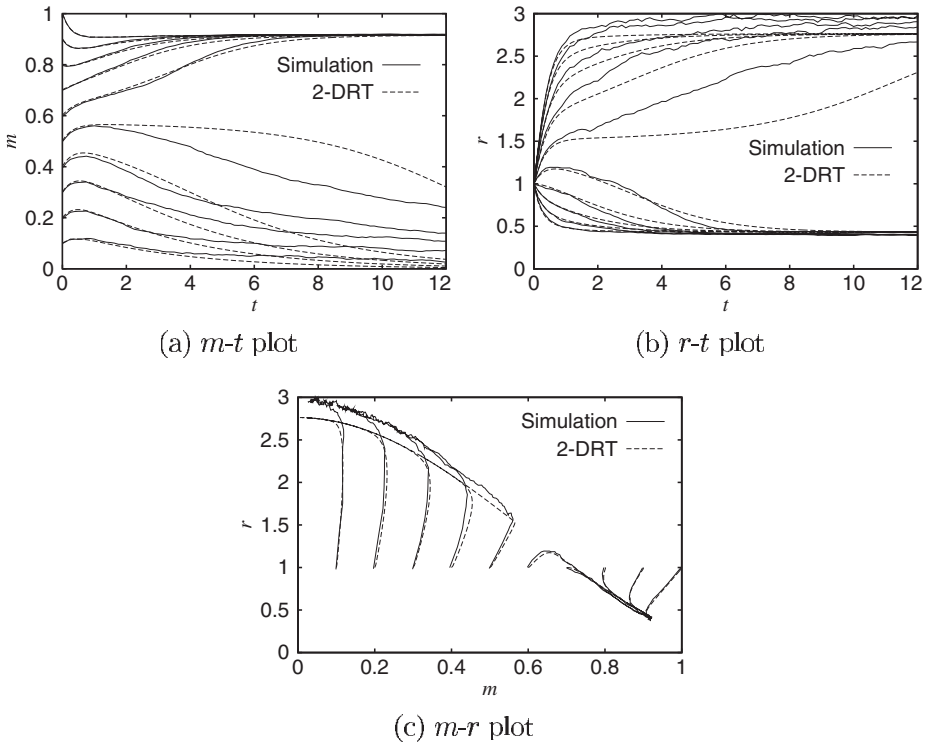

Figure 2. Dynamics obtained by simulations with $N = 2^{15}$ (solid curves) and computed by 2-DRT (dashed curves) for the case with $\alpha = 0.2$ and $\theta = 1.4$.

where $b \equiv \mu/\rho - m$. It has been shown that the (m, r)-annealing executes Monte Carlo sampling from a (m, r)-subshell with uniform probability (in the limit $N \to \infty$), hence realizing the equipartitioning. It is useful in investigating the validity of the equipartitioning assumption, and will be utilized in this paper.

4. Results

4.1. The time evolution of the order parameters

We first examined whether 2-DRT describes the overall characteristics of the dynamics of the non-monotonic model. We assume the common convention that initial microscopic states of the model are given by randomly corrupting the nominated pattern; that is, the initial state $\boldsymbol{s}$ is set by the probability law $\text{Prob}[s_i] = \delta(s_i - \xi_i^1)(1 + m_0)/2 + \delta(s_i + \xi_i^1)(1 - m_0)/2$, so that the initial overlap $m(t = 0)$ approximately equals to m_0 when N is sufficiently large. Following this initialization procedure, the initial value of r, when N is sufficiently large, approximately equals 1. We found that 2-DRT does describe the dynamics of the model considerably well, as shown in figure 2 for the case with $\alpha = 0.2$ and $\theta = 1.4$. 2-DRT reproduced the trajectories almost exactly when retrieval succeeded. Noticeable disagreement between simulations and 2-DRT was seen for cases where retrieval failed. The characteristic aspect of the disagreement is that the trajectories predicted by 2-DRT exhibit, in early stages, overall slowing down against the corresponding simulations. These observations are essentially the same as those found in the conventional model [8, 11, 13]. The observed disagreement is due to the failure of the

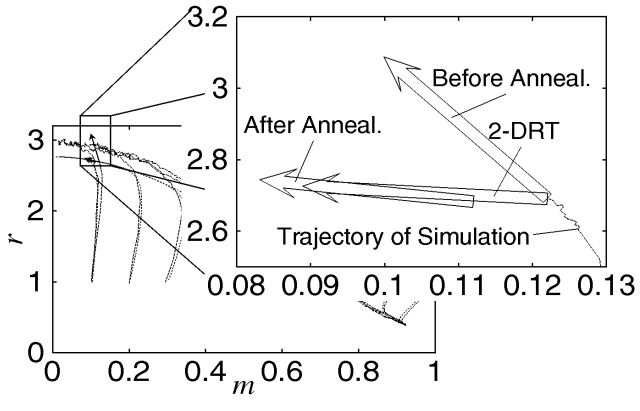

Figure 3. Flow vectors $(\dot{m}, \dot{r})$ at $t = 1$ on the trajectory starting at $(m, r) = (0.1, 1)$ for the model with $\alpha = 0.2$, $\theta = 1.4$ and $N = 2^{15}$. Three flow vectors, ones before and after the (m, r)-annealing, and one computed by 2-DRT, are shown.

equipartitioning assumption of 2-DRT just as in the conventional model, as demonstrated by the following numerical experiment. The procedure followed in this experiment is as follows: simulate a model with $\theta = 1.4$ and $\alpha = 0.2$ by setting its initial condition as $(m, r) = (0.1, 1)$, stop it at $t = 1$, and then execute the (m, r)-annealing for 80 time units. The flow vectors $(\dot{m}, \dot{r})$, evaluated from (1) the model just before executing the (m, r)-annealing, (2) the model just after it, and (3) 2-DRT, were compared, and the result is summarized in figure 3. This shows that the flow vectors of the model after the (m, r)-annealing and of 2-DRT are almost the same, whereas the flow vector before the (m, r)-annealing is different from these two, which means that the equipartitioning assumption does not hold in this case.

4.2. Capacity and basins of attraction

In this paper, we define the storage capacity α_c as the maximum value of α for which a stable macroscopic state with nonvanishing m exists. We call an equilibrium macroscopic state with nonvanishing m the retrieval state. Since the retrieval state may be unstable, the condition for the existence of a retrieval state will give an overestimate of the true storage capacity. On the other hand, a stable retrieval state may have a very small basin of attraction, so that we may fail to find such a retrieval state in numerical experiments even though it is stable.

Shiino and Fukai [2] have analysed equilibrium properties of continuous-valued continuous-time non-monotonic models using SCSNA. Although we consider the model with binary variables in this paper rather than ones with continuous values, the equilibrium condition is shown to be the same as that for the continuous-value continuous-time model owing to the current choice of the output function f (equation (3)), and thus SCSNA can be applied to the model treated here. We executed the SCSNA calculation on this model, and figure 4 shows the result for α_e, the maximum of α for which a retrieval state exists, versus θ. When $\theta \to \infty$, α_e approaches the well known value 0.138, confirming that SCSNA is consistent with the Amit–Gutfreund–Sompolinsky (AGS) theory [15]. As θ becomes smaller, α_e increases so that it reaches its maximal value $\alpha_e = 0.489$ at $\theta \approx 0.7$.

As we have already discussed, α_e gives an overestimation of the true storage capacity α_c [2]. To evaluate α_c itself, we have to take into account the dynamical aspect of the retrieval process. This discussion leads us to the idea of applying 2-DRT to determine the storage capacity α_c, by

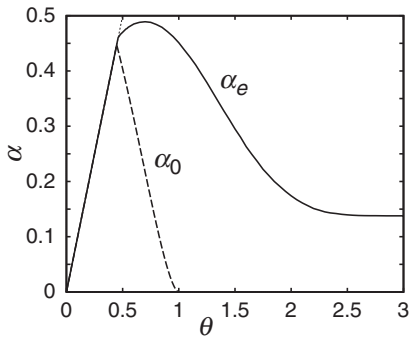

Figure 4. Plot of α_e, the maximum of α for which a retrieval state exists (solid curve), and critical capacity α_0 (dashed curve), under which super-retrieval occurs, against θ, evaluated by SCSNA calculation. The thin dashed line shows $\alpha = \theta$, which limits the capacity in the small-θ region.

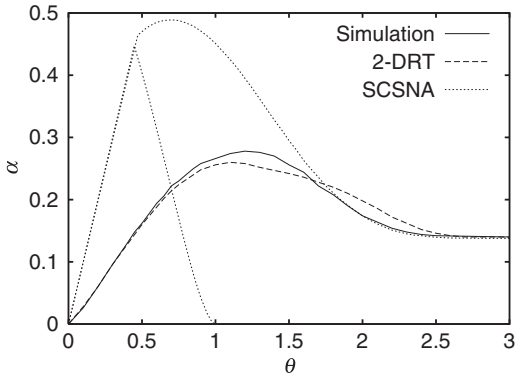

Figure 5. Plot of storage capacity α_c against θ, evaluated by simulation (solid curve) and by 2-DRT trajectory tracking (dashed curve). Plots of α_e and α_0 evaluated by SCSNA (shown in figure 4) are also shown for comparison.

observing whether or not the trajectories from arbitrary initial conditions approach a retrieval state.

Two points have to be mentioned here. First, although 2-DRT becomes exact at equilibrium for the conventional model [10, 11], it is no longer so for the non-monotonic model, which means that 2-DRT may not reproduce the storage capacity. Second, since we assume the initialization procedure described above, only the retrieval states which can be reached from the initial conditions with $r = 1$ are to be observed in the simulations. To correspond with this experimental setup, we estimated the storage capacity α_c by tracking 2-DRT trajectories from initial conditions with $r = 1$. The storage capacity estimated by the simulations and by the 2-DRT trajectory tracking may be therefore an underestimate against the *true* storage capacity, because there might be stable retrieval states unreachable from any initial condition with $r = 1$ (see section 4.3).

Figure 5 shows the estimated storage capacity α_c by 2-DRT trajectory tracking and by simulations. It can be seen that 2-DRT trajectory tracking reproduces well the storage capacity obtained by the simulations for the whole range of θ. Comparing it with figure 4 reveals that, while the agreement is good when θ is large, the discrepancy becomes apparent as θ becomes less than about 1.5, showing that the storage capacity estimated by 2-DRT is considerably smaller than that estimated by SCSNA. It may be partly explained by the overestimation of SCSNA described above.

One of the main advantages of dynamical theory is that it allows us to evaluate basins of attraction, because they are essentially of dynamical nature. We used 2-DRT to evaluate the basin of attraction of the retrieval states. Since we adopt the above-mentioned initialization convention, we consider the basin of attraction as being represented in terms of m only, that

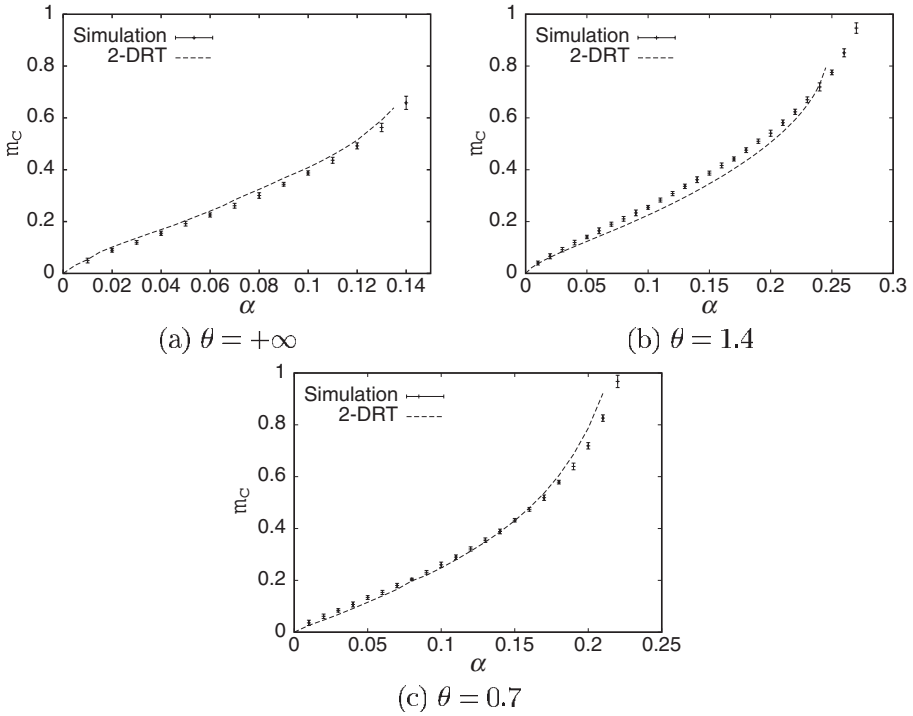

Figure 6. Plot of critical initial overlap m_c against α, evaluated by 2-DRT (solid curve) and by simulation (markers) for $\theta = +\infty$, 1.4 and 0.7.

is, we regard a value of m_0 as belonging to the basin of attraction of the retrieval state if the trajectory starting at the state $(m,\ r) = (m_0,\ 1)$ approaches the retrieval state. Evaluating the basin of attraction defines the critical initial overlap m_c, which means that initial states $(m_0,\ 1)$ with $m_0 \geqslant m_c$ yield successful retrieval. Figures 6 and 7 show the critical initial overlap m_c and the values of m of the retrieval state, respectively, evaluated by 2-DRT and by simulations. It is readily seen that enlargement of the basin of attraction occurs as θ becomes small, and that 2-DRT captures this phenomenon reasonably well.

4.3. Super-retrieval states

As a result of SCSNA analysis on non-monotonic models, Shiino and Fukai [2] have shown that there is a phase where equilibrium states corresponding to 'perfect' retrieval exist. Such states are called the super-retrieval states, whose existence is one of unique features of the non-monotonic models. Here, 'perfect' means that the correlation of the sign of the local field $h_i(s)$ (not of s) with the nominated pattern $\boldsymbol{\xi}^1$ is exactly equal to ± 1. The correlation defined as above is called the tolerance overlap [2]. The critical capacity α_0, below which the super-retrieval occurs, can be evaluated numerically by SCSNA, and is also shown in figure 4.

An explanation, given by Shiino and Fukai [2], for the possible existence of such states is briefly as follows: for such states $r_{\mathrm{AGS}} \to +0$ holds, which has been confirmed by numerically solving relevant self-consistent equations. Since variance of the noise term (without the 'systematic' term, ΓY, in their terminology [2]) is given by αr_{AGS} in SCSNA, it implies that the effect of the noise completely vanishes in the states, which enables the super-retrieval.

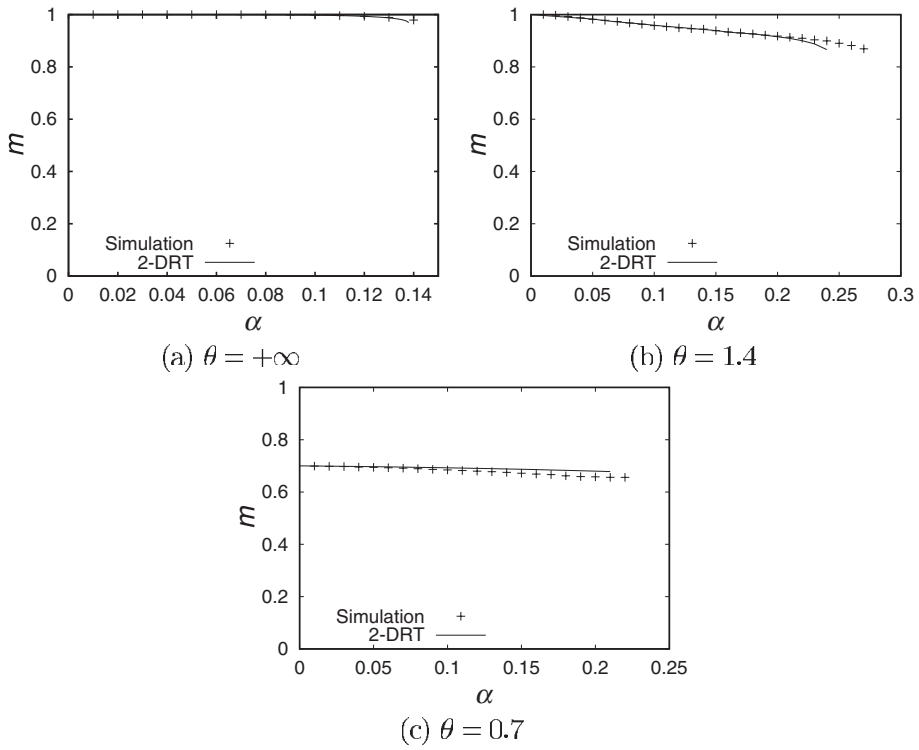

Figure 7. Plot of the value of m of the retrieval state against α, evaluated by 2-DRT (solid curve) and by simulation (markers) for $\theta = +\infty$, 1.4 and 0.7.

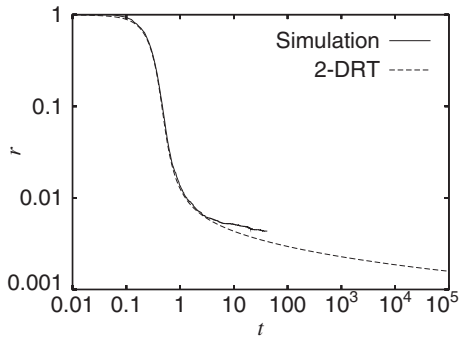

Figure 8. Time evolution of r for $\theta = 0.4$, $\alpha = 0.05$, and with initial condition $m_0 = 0.9$, evaluated by simulation with $N = 2^{15}$ (solid curve) and by 2-DRT (dashed curve).

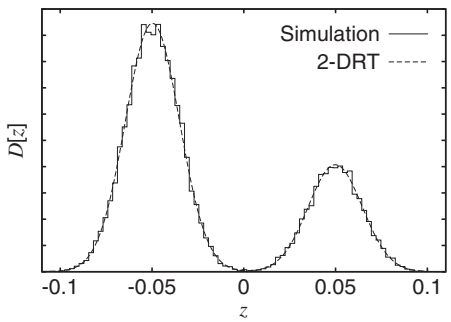

Figure 9. Noise distribution $D[z]$ at the equilibrium state $((m,\ r) = (0.398,\ 0.004\,40))$ achieved by the simulation with $\theta = 0.4$, $\alpha = 0.05$, $N = 2^{15}$, and initial condition $m_0 = 0.9$ (solid curve), and the one computed by 2-DRT for the same values of $(m,\ r)$ (dashed curve).

Especially interesting is whether or not 2-DRT provides an appropriate description of dynamics which is bound for super-retrieval states. To see this, we examined the case where $\theta = 0.4$ and $\alpha = 0.05$, which, according to SCSNA analysis, is expected to have the super-retrieval states. Figure 8 shows the time evolution of r evaluated by simulation and by 2-DRT, with initial condition $m_0 = 0.9$. Again, 2-DRT reproduced the simulation result fairly

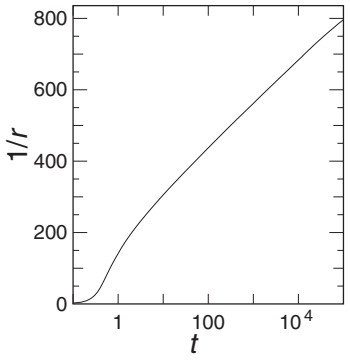

Figure 10. Plot of $1/r$ versus $\ln t$ for $\theta = 0.4$, $\alpha = 0.05$, and with initial condition $m_0 = 0.9$, evaluated by 2-DRT.

well. For the simulation, state transition ended (confirmed numerically) at $t \approx 30$, where $(m,\ r) = (0.398,\ 0.004\,40)$. The tolerance overlap was evaluated to be exactly equal to 1 at this state, indicating that this is the super-retrieval state. Figure 9 shows the noise distribution $D[z]$ at the equilibrium state achieved by the simulation, and the one computed by 2-DRT for the same values of $(m,\ r)$. They are in good agreement, suggesting that 2-DRT can successfully predict the trajectories even in the case of super-retrieval, provided that the system size N is sufficiently large. As for 2-DRT, the value of r continued to decrease at $t \approx 10^5$ (we stopped computation of 2-DRT at $t = 10^5$ because rounding errors became profound beyond this point), where $(m,\ r) = (0.399,\ 0.001\,59)$. We observed numerically that t-dependence of the decrease of r can be expressed, to a good approximation, as $r(t) \propto 1/\ln t$ (figure 10), which strongly supports the conjecture that the trajectory obtained by 2-DRT certainly approaches $r = 0$. As can be seen by equation (8), variance of the noise term is, roughly speaking, given by αr in 2-DRT. Then, if the super-retrieval states are described appropriately by 2-DRT, they should correspond to the states with $r = +0$. In the following we therefore investigate the solutions of the saddle-point equations (11) when $r = +0$.

By formally taking the limit $r \to +0$, the saddle-point equations (11) are reduced to the following equations:

$$\rho = -\infty \tag{13}$$

$$m = \int Dy\ \tanh(\lambda y + \mu) \tag{14}$$

$$q = \int Dy\ \tanh^2(\lambda y + \mu) \tag{15}$$

$$\lambda = -\frac{\sqrt{\alpha q}}{1-q} \tag{16}$$

and, correspondingly, the RS noise distribution $D^{\mathrm{RS}}_{m,\,r=+0}[z]$ (8) becomes

$$D^{\mathrm{RS}}_{m,\,r=+0}[z] = \frac{1-m}{2}\delta(z-\alpha) + \frac{1+m}{2}\delta(z+\alpha). \tag{17}$$

The condition that the macroscopic state $(m,\ r = +0)$ is an equilibrium state, that is, $(\dot{m},\ \dot{r}) = (0,\ 0)$ holds, is thus given by

$$f(m \pm \alpha) = \mp 1. \tag{18}$$

For the current choice of the function f (equation (3)), this condition is satisfied when $0 < m - \alpha < \theta < m + \alpha$, or equivalently, $\max\{\theta - \alpha,\ \alpha\} < m < \min\{\theta + \alpha,\ 1\}$. This is consistent with the observation from the simulations that m tends to approach θ when the super-retrieval occurs.

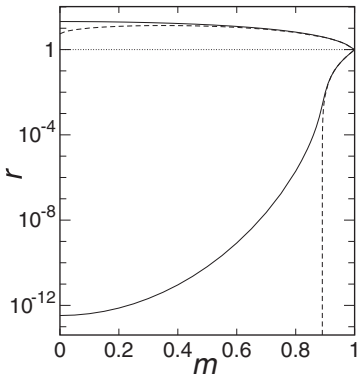

Figure 11. The freezing line (solid curve) and the AT line (dashed curve) for $\alpha = 0.05$.

One may notice that the RS noise distribution $D^{\mathrm{RS}}_{m,\,r=0}[z]$ (equation (8)), whose components are delta functions and hence have zero width, seems incompatible with the noise distribution at the super-retrieval state observed in the simulation (figure 9), which has two components with finite width. However, this is ascribed to the finite-size effect, as discussed later.

The applicability of 2-DRT depends not only on the two assumptions made at the beginning but also on the two following points: the first one concerns the so-called freezing line, which defines the points in the $(m,\ r)$ plane where the number of microscopic states within the $(m,\ r)$-subshell changes from an exponentially large number to an exponentially small number in terms of N. The second one concerns the so-called de Almeida–Thouless (AT) line [18], at which the replica-symmetry-breaking (RSB) occurs and thus the RS ansatz becomes no longer valid. These two points should be addressed in order to assess the validity of taking the formal limit $r \to +0$ in the 2-DRT framework.

When N is large, the number of microscopic states within $(m,\ r)$-subshell is scaled as $\mathrm{e}^{N\nu(m,r)}$. The exponent $\nu(m,\ r)$ is given, under the RS ansatz, by the following formula [11]:

$$\nu(m,\ r) = \int Dy \ln\cosh\left[\lambda y + \mu\right] - \mu m - \frac{\alpha}{2}\left[\ln[1-\rho(1-q)] + \frac{\rho(1-q)(1-\rho+3q\rho)}{[1-\rho(1-q)]^2}\right] + \ln 2. \tag{19}$$

The condition $\nu(m,\ r) = 0$ defines the freezing line. The number of microscopic states within the subshell is exponentially large, and therefore taking averages over the subshell is expected to have the proper meaning, as long as $\nu(m,\ r)$ is positive. For $r = 1$ and $|m| < 1$, $\nu(m,\ r)$ becomes

$$\nu(m,\ r=1) = -\frac{1}{2}\left[(1+m)\ln\frac{1+m}{2} + (1-m)\ln\frac{1-m}{2}\right] > 0 \tag{20}$$

so that the number of microscopic states is indeed exponentially large. In the limit $r \to +0$, however, $\nu(m,\ r)$ goes to $-\infty$, implying that $r = 0$ is outside the freezing line. This means that there are so few microscopic states near $r = 0$, which may in part explain the observation from the simulations that the trajectories approaching $r = 0$ reach equilibrium before actually arriving at $r = 0$. That $r = 0$ is outside the freezing line also means that the argument with the formal limit $r \to +0$ eventually loses its proper meaning, because the relevant subshell average is over an *exponentially small* number of microscopic states. Numerical evaluation reveals, however, that the freezing line for $r < 1$ lies very close to $r = 0$ (figure 11). This shows that the number of microscopic states, having vanishing—not exactly zero—overlaps with non-nominated patterns $\boldsymbol{\xi}^{\mu}$, $\mu > 1$, while keeping the overlap with the nominated pattern

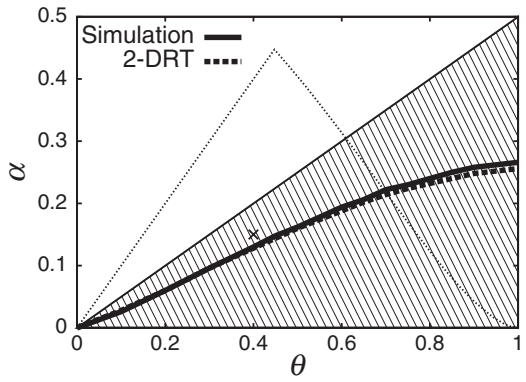

Figure 12. The region where the super-retrieval solution $(m,\ r) = (\theta,\ 0)$ is stable, evaluated by 2-DRT local stability analysis (shaded region), by tracking simulation trajectories (the region below the thick solid curve) and by tracking 2-DRT trajectories (the region below the thick dashed curve). The region where super-retrieval state exists, evaluated by SCSNA (see figure 4) is also shown (dotted) for comparison.

ξ^1 high, is indeed *large*. (This is nontrivial because we are working with the *discrete* state space $\{-1,\ 1\}^N$.) Moreover, the saddle-point solution of the order parameters changes smoothly as r tends to +0: let μ_0, q_0 be the asymptotic values of the saddle-point solution μ, q, respectively. Then the asymptotic form of the saddle-point solution as $r \to +0$ is given by

$$\begin{aligned} \rho &= -r^{-1} + \mathrm{O}(1) \\ \lambda &= -\frac{\sqrt{\alpha q_0}}{1-q_0} + \mathrm{O}(r) \\ \mu &= \mu_0 + \mathrm{O}(r) \\ q &= q_0 + \mathrm{O}(r) \\ \Delta &= -\alpha + \mathrm{O}(r) \end{aligned} \tag{21}$$

which shows that the solution exhibits any anomalous behaviour around $r = 0$. We can therefore expect that the argument presented above on the formal limit $r \to +0$ captures well qualitative aspects of the equilibrium states achieved by the simulations.

The AT line is determined by examining the stability of the RS solution. Assuming that RSB is caused by destabilization of the so-called 'replicon' modes [16–18] for the case $r < 1$ just as it has been assumed for the case $r \geqslant 1$ [11], the AT line turns out to be given by the same formula as given in [11] for $r \geqslant 1$:

$$\alpha = \rho^2(\alpha + \Delta)^2 \int \frac{Dy}{\cosh^4(\lambda y + \mu)}. \tag{22}$$

The RS solution is valid if the right-hand side of equation (22) is less than α. We confirmed that, for the case where $\alpha = 0.05$, the AT line lies in the region $m > 0.890$ for $r < 1$ (figure 11), which implies that the super-retrieval observed in the simulations was irrelevant to RSB.

We have performed local stability analysis of the 2-DRT stationary solutions $r = 0$, $\max\{\theta - \alpha,\ \alpha\} < m < \min\{\theta + \alpha,\ 1\}$ corresponding to the super-retrieval state. The result of the analysis states that, among the super-retrieval solutions, $(m,\ r) = (\theta,\ 0)$ is the only attractor when $2\alpha < \theta < 1$, although it becomes unstable when $\alpha < \theta < \min\{2\alpha,\ 1\}$. For the details of the local stability analysis, see the appendix. In the simulations, however, it is not for all $(\theta,\ \alpha)$ values satisfying $2\alpha < \theta < 1$ that the super-retrieval was observed. Figure 12 shows the region where the local stability analysis of the 2-DRT predicts the stable super-retrieval

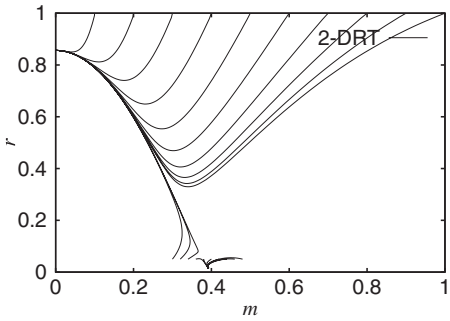

Figure 13. Trajectories predicted by 2-DRT in $(m,\ r)$ plane with $(\theta,\ \alpha) = (0.4,\ 0.15)$.

state, the one where the super-retrieval is observed by simulations (in the sense that tolerance overlap is numerically evaluated to be 1), and the one where the super-retrieval is predicted by tracking the 2-DRT trajectories starting at $(m,\ r) = (m_0,\ 1)$. The second and third regions are in good agreement with each other. Both are within the first region, the region where the super-retrieval state is locally stable, as they should be, but apparently they do not coincide with the first one. The region where the super-retrieval is observed in simulations may be further affected by the following factors:

- The super-retrieval solution $(m,\ r) = (\theta,\ 0)$ may not be reachable from the conventional initial states with $r = 1$, even though it is an attractor.
- Even if the stable super-retrieval solution $(m,\ r) = (\theta,\ 0)$ exists, the system may be equilibrated at a state with a nonzero r value, where tolerance overlap is exactly 1, due to the finite-size effect.
- The super-retrieval solution $(m,\ r) = (\theta,\ 0)$ may be at the outside of the RS region, where the stationarity and local stability arguments, both based on the RS ansatz, are no longer valid.

A demonstration regarding the first factor is shown in figure 13. For the condition $(\theta,\ \alpha) = (0.4,\ 0.15)$ (marked by a cross in figure 12), for example, the super-retrieval state is not observed by following time evolution by either numerical simulation or 2-DRT. Nevertheless, 2-DRT predicts that under this condition the stable super-retrieval state exists at $(m,\ r) = (0.4,\ 0)$. As shown in the figure, 2-DRT trajectory tracking shows that in this condition the super-retrieval state is indeed stable, but it is not reachable from the initial states with $r = 1$. Therefore, the difference in the upper-α boundary of the regions obtained by 2-DRT local stability analysis and by trajectory tracking is explained by the first factor.

As for the finite-size effect, we have already shown a simulation result in which the system is equilibrated and the tolerance overlap is exactly 1, while $r = 0.004\,40 > 0$ (figure 8) and the two components of the noise distribution remain of finite width (figure 9). Theoretically, the width of the components should go down to 0 in order for the system to arrive at the stable super-retrieval state, because the tolerance overlap g is given by

$$g = 1 - \int_{-\infty}^{-m} D_{m,\,r}[z] \tag{23}$$

which equals 1 only when the left tail of the noise distribution $D_{m,\,r}[z]$ vanishes, and because the driving force to decrease r is provided by the tails of the noise distribution, if they exist, as discussed in the appendix. In the simulations, on the other hand, it may happen that none of the realizations z_i of the noise (there are N realizations of the noise for a system with N units) falls into the tail regions, even though r is positive and thus the noise distribution has finite weight at the tails. In such cases, the tolerance overlap will become exactly 1 and time

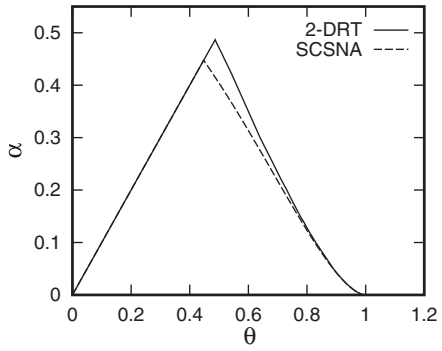

Figure 14. The region where, according to 2-DRT, the super-retrieval solution $(m,\ r) = (\theta,\ 0)$ is a stationary point and satisfies the RS ansatz (solid curve) and the super-retrieval phase evaluated by SCSNA (dashed curve). The right solid curve corresponds to the AT line.

evolution will stop before r becomes exactly 0. This is the reason why the tolerance overlap can take the value 1 while the system is equilibrated at a state with nonzero r. We also found that this finite-size effect made it difficult to determine by simulations the boundary at the large-θ side of the region where super-retrieval occurs (figure 12): the region where super-retrieval occurs, evaluated by simulations, extended beyond the theoretical upper bound $\theta = 1$, and the boundary at the large-θ side was sensitive to N even though N was taken as large as 2^{15} in our study, indicating that this is indeed the finite-size effect.

Concerning the last factor, we have demonstrated that the super-retrieval state attained by the simulation shown in figure 8 was irrelevant to RSB. However, as shown in figure 11 the AT line goes across $r = 0$ at $m \sim 0.89 < 1$ for $\alpha = 0.05$ for example, implying that it *is* relevant when θ is closer to 1. In order to investigate the last factor rigorously, 2-DRT analysis taking RSB into account would be required, which is technically too complicated to be treated in this paper. Instead, we would like to mention an interesting observation related to the last factor: there is a rough numerical correspondence between the region where the equilibrium super-retrieval solution $(m,\ r) = (\theta,\ 0), \alpha < \theta < 1$, which may not be stable, satisfies the RS ansatz, and the region where SCSNA predicts super-retrieval to occur, as shown in figure 14. Because of RSB, as well as the finite-size effect, it is extremely difficult to determine both theoretically and numerically the boundary at the large-θ side of the region where super-retrieval occurs.

5. Conclusion

We have studied the question of how well 2-DRT describes retrieval dynamics of the non-monotonic model. Although there is no theoretical justification for 2-DRT to be exact either for the non-monotonic model, 2-DRT turns out to reproduce the retrieval dynamics quite well, and it also gives reasonable results for the capacity, basins of attractions and the super-retrieval states.

Appendix. Local stability analysis of super-retrieval states

We first split the RS noise distribution $D^{\mathrm{RS}}_{m,\,r}[z]$ into two components, as follows:

$$D^{\mathrm{RS}}_{m,\,r}[z] \equiv D^{-}[z] + D^{+}[z] \tag{24}$$

$$D^{\pm}[z] = \frac{\mathrm{e}^{-(\Delta \pm z)^2/2\alpha r}}{2\sqrt{2\pi\alpha r}} w_{\pm}(z) \tag{25}$$

$$w_{\pm}(z) = 1 - \int Dy\ \tanh\left[\lambda y \left(\frac{\Delta}{\rho\alpha r}\right)^{1/2} + (\Delta \pm z)\rho\frac{r_{\mathrm{AGS}}}{r} \pm \mu\right]. \tag{26}$$

Note that $w^{\pm}(z)$ is 'slowly varying' with respect to z, because

$$\left|\frac{\mathrm{d}w^{\pm}(z)}{\mathrm{d}z}\right| < \left|\rho\frac{r_{\mathrm{AGS}}}{r}\right| \tag{27}$$

holds and the bound $|\rho r_{\mathrm{AGS}}/r|$ remains finite even when $r \to +0$. We can thus regard that each component is basically a Gaussian distribution centred at $z = \mp\Delta$ and width $\mathrm{O}(\sqrt{\alpha r})$, and it has been modulated by a bounded, monotonic, and slowly varying function $0 < w_{\pm}(z) < 2$. From the asymptotic form of the saddle-point solution as $r \to +0$ (equation (21)), we can expect, for small r, that the noise components $D^{\pm}[z]$ become sharply peaked around $z = \mp\Delta \approx \pm\alpha$. In the limit $r \to +0$, we have

$$D^{\pm}[z] = \frac{1 \mp m}{2}\delta(z \mp \alpha) \tag{28}$$

so that the condition

$$\max\{\theta - \alpha,\ \alpha\} < m < \min\{\theta + \alpha,\ 1\} \tag{29}$$

is obtained for the existence of equilibrium states of the form $(m,\ r) = (m,\ 0)$, as discussed in section 4.3.

In this section we analyse local stability of the equilibrium states $(m,\ r = 0)$ satisfying the condition (29). Using the noise components, the time evolution equations are rewritten as

$$\begin{aligned}
\dot{m} &= \int_{-\infty}^{\infty}\mathrm{d}z\, D^{-}[z]\, f(m+z) + \int_{-\infty}^{\infty}\mathrm{d}z\, D^{+}[z]\, f(m+z) - m \\
\frac{1}{2}\dot{r} &= \frac{1}{\alpha}\left[\int_{-\infty}^{\infty}\mathrm{d}z\, D^{-}[z]\, z f(m+z) + \int_{-\infty}^{\infty}\mathrm{d}z\, D^{+}[z]\, z f(m+z)\right] + 1 - r.
\end{aligned} \tag{30}$$

Because $D^{\pm}[z]$ are sharply peaked, as the first step of approximation we can assume that $f(m+z) = f(m \mp \Delta)$ in the integrals with $D^{\pm}[z]$. This assumption becomes exact in the limit $r \to +0$ and when $f(m+z)$ is continuous around $z = \pm\alpha$, but for finite r it gives an approximate result and the approximation error comes from the contribution of the *tails* of $D^{\pm}[z]$ where $f(m+z)$ changes the sign. For explanation purposes we introduce the following four regions:

$$\begin{aligned}
&\mathrm{I} \equiv \{z \mid m + z < -\theta\} \\
&\mathrm{II} \equiv \{z \mid -\theta < m + z < 0\} \\
&\mathrm{III} \equiv \{z \mid 0 < m + z < \theta\} \\
&\mathrm{IV} \equiv \{z \mid \theta < m + z\}.
\end{aligned} \tag{31}$$

$f(m+z) = 1$ for $z \in$ I or III, and $f(m+z) = -1$ for $z \in$ II or IV. The equilibrium states which we are interested in correspond to the case where the peak of $D^{+}[z]$ is in the region IV and that of $D^{-}[z]$ in the region III. In this case the time evolution equations are approximated to be

$$\begin{aligned}
\dot{m} &\approx \int_{-\infty}^{\infty}\mathrm{d}z\, D^{-}[z] - \int_{-\infty}^{\infty}\mathrm{d}z\, D^{+}[z] - m \\
\frac{1}{2}\dot{r} &\approx \frac{1}{\alpha}\left[\int_{-\infty}^{\infty}\mathrm{d}z\, D^{-}[z]\, z - \int_{-\infty}^{\infty}\mathrm{d}z\, D^{+}[z]\, z\right] + 1 - r.
\end{aligned} \tag{32}$$

However, direct calculation shows that the right-hand sides of these equations exactly equal to 0. This fact indicates that the time evolution near $r = 0$ should be governed by the contribution of the *tails*.

The principal contribution comes from the largest one of the following three quantities:

(1) Contribution of the tail of $D^+[z]$ in the region III:

$$I_1 = 2\int_{\mathrm{III}} \mathrm{d}z\, D^+[z]\, a(z) \approx 2\int_{-\infty}^{z_0} \mathrm{d}z\, D^+[z]\, a(z) \tag{33}$$

(2) Contribution of the tail of $D^-[z]$ in the region IV:

$$I_2 = -2\int_{\mathrm{IV}} \mathrm{d}z\, D^-[z]\, a(z) = -2\int_{z_0}^{\infty} \mathrm{d}z\, D^-[z]\, a(z) \tag{34}$$

(3) Contribution of the tail of $D^-[z]$ in the region II:

$$I_3 = -2\int_{\mathrm{II}} \mathrm{d}z\, D^-[z]\, a(z) \approx -2\int_{-\infty}^{-m} \mathrm{d}z\, D^-[z]\, a(z) \tag{35}$$

where $z_0 \equiv \theta - m$, and $a(z) = 1$ or z, depending on which of $\dot{m}$ and $\dot{r}$ we are considering. We approximate each contribution by extending the integral region to ∞ or $-\infty$. In fact this approximation does not affect the final result in the $r \to +0$ limit because it changes each quantity by a vanishingly small amount.

First let us consider the contribution to $\dot{m}$. Evaluation for I_1 yields

$$\begin{aligned} I_1 &\approx 2\int_{-\infty}^{z_0} \mathrm{d}z\, D^+[z] \\ &= \int_{-\infty}^{z_0} \mathrm{d}z \frac{\mathrm{e}^{-(\Delta+z)^2/2\alpha r}}{\sqrt{2\pi\alpha r}} w_+(z) \\ &\approx \int_{-\infty}^{z_0} \mathrm{d}z \frac{\mathrm{e}^{-(\Delta+z)^2/2\alpha r}}{\sqrt{2\pi\alpha r}} w_+(z_0) \\ &\approx \frac{1}{\sqrt{2\pi}} \exp\left[-\frac{(z_0+\Delta)^2}{2\alpha r} - \ln\frac{z_0+\Delta}{\sqrt{\alpha r}} + \ln w_+(z_0)\right]. \end{aligned} \tag{36}$$

Similarly, for I_2 and I_3, we have

$$I_2 \approx -\frac{1}{\sqrt{2\pi}} \exp\left[-\frac{(z_0-\Delta)^2}{2\alpha r} - \ln\frac{z_0-\Delta}{\sqrt{\alpha r}} + \ln w_-(z_0)\right] \tag{37}$$

$$I_3 \approx -\frac{1}{\sqrt{2\pi}} \exp\left[-\frac{(-m-\Delta)^2}{2\alpha r} - \ln\frac{-m-\Delta}{\sqrt{\alpha r}} + \ln w_-(-m)\right] \tag{38}$$

respectively. In the $r \to +0$ limit, the dominant contribution comes from the first term of the exponent for each case, so that comparison of the term is sufficient to determine which of I_1, I_2 and I_3 has the largest contribution to $\dot{m}$. The result of the comparison for small r is summarized as follows:

- When $-2\Delta < \theta$, the largest contribution comes from I_1 or I_2. If $m < \theta$, I_1 is the largest and $\dot{m} > 0$. Otherwise, I_2 is the largest and $\dot{m} < 0$.
- When $-2\Delta > \theta$, the largest contribution comes from I_2 or I_3. Since both I_2 and I_3 have negative contribution, $\dot{m} < 0$.

From this result, we can conclude that the stable super-retrieval state, if it exists, should be $(m, r) = (\theta, 0)$, and that $2\alpha < \theta < 1$ is a necessary condition for the existence of the stable super-retrieval state.

Let us now take a closer look at the flow near the state $(m, r) = (\theta, 0)$. We let $\varepsilon \equiv -z_0 = m - \theta$, and consider time evolution of the two small quantities, ε and r. In

the following arguments we assume that $-2\Delta < \theta$ holds, so that the principal contribution comes from I_1 or I_2, but not from I_3. Under this assumption, we have

$$\begin{aligned}\dot{\varepsilon} &\approx \sqrt{\frac{2\alpha r}{\pi}}\mathrm{e}^{-(\Delta^2+\varepsilon^2)/2\alpha r}\bar{w}\Big(-\frac{1}{\Delta}\Big)\Big[\tanh\frac{\Delta\varepsilon}{\alpha r}+\frac{\delta}{\bar{w}}\Big]\cosh\frac{\Delta\varepsilon}{\alpha r}\\ \frac{1}{2}\dot{r} &\approx \sqrt{\frac{2\alpha r}{\pi}}\mathrm{e}^{-(\Delta^2+\varepsilon^2)/2\alpha r}\bar{w}\Big(\frac{r}{\Delta^2}\Big)\Big[\Big(\frac{\Delta\varepsilon}{\alpha r}-\frac{\delta}{\bar{w}}\Big)\tanh\frac{\Delta\varepsilon}{\alpha r}+\Big(\frac{\delta}{\bar{w}}\frac{\Delta\varepsilon}{\alpha r}-1\Big)\Big]\cosh\frac{\Delta\varepsilon}{\alpha r}\end{aligned} \tag{39}$$

where

$$\begin{aligned}\bar{w} &\equiv \tfrac{1}{2}\big(w_+(z_0)+w_-(z_0)\big)\\ \delta &\equiv \tfrac{1}{2}\big(w_+(z_0)-w_-(z_0)\big).\end{aligned} \tag{40}$$

Note that $-1 < \delta/\bar{w} < 1$ holds.

Assuming that ε/r remains finite, we can readily see that $\dot{r}$ is smaller in magnitude than $\dot{\varepsilon}$ by a factor r. Then for small enough r the slaving principle applies and ε is expected to relax toward its equilibrium value much faster than r. This justifies the adiabatic approximation, and we can regard that the equilibrium condition for ε,

$$\tanh\frac{\Delta\varepsilon}{\alpha r}+\frac{\delta}{\bar{w}}=0 \tag{41}$$

holds throughout the dynamics. This is indeed consistent with the assumption that ε/r remains finite. $\dot{r}$ is then given by

$$\frac{1}{2}\dot{r} \approx -\sqrt{\frac{2\alpha r}{\pi}}\mathrm{e}^{-(\Delta^2+\varepsilon^2)/2\alpha r}\bar{w}\Big(\frac{r}{\Delta^2}\Big)\Big[1-\Big(\frac{\delta}{\bar{w}}\Big)^2\Big]^{1/2} < 0. \tag{42}$$

This shows that the state $(m,\ r) = (\theta,\ 0)$ is actually a stable point of the dynamics described by 2-DRT under the condition $2\alpha < \theta < 1$.

References

[1] Morita M 1993 Associative memory with nonmonotone dynamics *Neural Networks* **6** 115–26

[2] Shiino M and Fukai T 1993 Self-consistent signal-to-noise analysis of the statistical behaviour of analog neural networks and enhancement of the storage capacity *Phys. Rev.* E **48** 867–97

[3] Rieger H, Schreckenberg M and Zittartz J 1988 Glauber dynamics of the Little-Hopfield model. *Z. Phys.* B **72** 523–33

[4] Gardner E, Derrida B and Mottishaw P 1987 Zero temperature parallel dynamics for infinite range spin glasses and neural networks *J. Physique* **48** 741–55

[5] Horner H, Bormann D, Frick M, Kinzelbach H and Schmidt A 1989 Transients and basins of attraction in neutral network models *Z. Phys.* B **76** 381–98

[6] Okada M 1995 A hierarchy of macrodynamical equations for associative memory *Neural Networks* **8** 833–8

[7] Amari S and Maginu K 1988 Statistical neurodynamics of associative memory *Neural Networks* **1** 63–73

[8] Nishimori H and Ozeki T 1993 Retrieval dynamics of associative memory of the Hopfield type *J. Phys. A: Math. Gen.* **26** 859–71

[9] Nishimori H and Opriş I 1993 Retrieval process of an associative memory with a general input–output function *Neural Networks* **6** 1061–7

[10] Coolen A C C and Sherrington D 1993 Dynamics of fully connected attractor neural networks near saturation *Phys. Rev. Lett.* **71** 3886–9

[11] Coolen A C C and Sherrington D 1994 Order-parameter flow in the fully connected Hopfield model near saturation *Phys. Rev.* E **49** 1921–34
(Erratum: Coolen A C C and Sherrington D 1994 *Phys. Rev.* E **49** 5906)

[12] Ozeki T and Nishimori H 1994 Noise distributions in retrieval dynamics of the Hopfield model *J. Phys. A: Math. Gen.* **27** 7061–8

[13] Tanaka T and Osawa S 1998 On macroscopic description of recurrent neural network dynamics *J. Phys. A: Math. Gen.* **31** 4197–202

[14] Coolen A C C and Franz S 1994 Closure of macroscopic laws in disordered spin systems: a toy model *J. Phys. A: Math. Gen.* **27** 6947–54
[15] Amit D J, Gutfreund H and Sompolinsky H 1985 Storing infinite numbers of patterns in a spin-glass model of neural networks *Phys. Rev. Lett.* **55** 1530–3
[16] Amit D J, Gutfreund H and Sompolinsky H 1987 Statistical mechanics of neural networks near saturation *Ann. Phys., NY* **173** 30–67
[17] Fischer K H and Hertz J A 1991 *Spin Glasses (Cambridge Studies in Magnetism vol 1)* (Cambridge: Cambridge University Press)
[18] de Almeida J R L and Thouless D J 1978 Stability of the Sherrington-Kirkpatrick solution of a spin glass model *J. Phys. A: Math. Gen.* **11** 983–90